Journal of Alloys and Compounds 489 (2010) 694–699

Contents lists available at ScienceDirect

Journal of Alloys and Compounds

journal homepage: www.elsevier.com/locate/jallcom

Preparation and DSC application of the size-tuned ZnO nanoarrays

Kaidi Yuan, Xin Yin, Jiangtian Li, Jianjun Wu, Yaoming Wang, Fuqiang Huang*

CAS Key Laboratory of Materials for Energy Conversion, Shanghai Institute of Ceramics, Chinese Academy of Sciences, 1295 Dingxi Road, Shanghai 200050, PR China

ARTICLE INFO

Article history:
Received 4 May 2009
Received in revised form
24 September 2009
Accepted 27 September 2009
Available online 9 October 2009

Keywords:
ZnO nanoarray
Seed crystal layer
Growth mechanism
Optical property

ABSTRACT

ZnO nanoarray was successfully prepared by a simple chemical bath deposition method on the glass slide deposited with a spin-coated ZnO seed crystal layer. With the measurements of SEM, XRD and UV–vis absorption spectra, the properties of the ZnO nanoarray were characterized in detail. The results show that the ZnO nanoarray is the hexagonal wurtzite structure and grow along the [0 0 1] axis. Furthermore, the energy-conversion property of the device was investigated in such ZnO nanoarray constructed dye-sensitized solar cells (DSCs), which has potential applications in the new-concept photovoltaic devices.

1. Introduction

Zinc oxide (ZnO), as a semiconductor with a wide band gap of 3.37 eV and the higher exciton binding energy (60 meV) at room temperature, has attracted great interest due to its special properties and potential applications in such fields as chemical sensors [1], dye-sensitized solar cells [2], nanogenerators [3], nanolasers [4], and transparent film coating [5].

Also, a lot of ZnO nanostructures have been reported, such as nanobelts [6], nanorings [7], nanohelices [8], nanotubes [9], nanorods or nanowires [10], and so forth. Among these one-dimensional structures, ZnO nanorods exhibit the promising application potentials, especially after the report of the room temperature ultraviolet lasing behavior [11]. To date, many methods to synthesize ZnO nanorods have been used, like metallorganic chemical vapor deposition (MOCVD) [12], a template-based method [13], laser ablation [14], spray pyrolysis technique [15], and solution methods [16,17]. Some extensive review articles summarized the most recent developments in the growth and applications of ZnO nanorods [18,19]. However, these methods are always limited by the disadvantages of high temperature, use of catalyst or carrier gas, expensive apparatus, low yield, the given substrate, and even the vacuum technique. Recently, a low temperature (below 100 °C), low cost, large scale, simple chemical bath deposition (CBD) method has been developed to synthesize the well-aligned zinc oxide nanoarrays. But few methods to tune the array size have been reported. It is well known that controlling the size of zinc oxide nanoarrays can greatly influence the performance of the final functional devices. So the size-tuned synthesis of the zinc oxide nanoarrays is in great demand. In this paper, we report the two-step synthesis of zinc oxide nanoarrays by a spin-coating method followed by a simple chemical bath deposition. Both glass slide and the fluorine-doped tin oxide conduction glass (FTO) were used as the substrates to grow the zinc oxide nanoarrays. The size of zinc oxide nanoarrays can be well tuned by varying the concentration of the precursor solution and the stirring time. Eventually, the as-prepared samples were utilized to construct the dye-sensitized solar cell, whose brief introduction is given in detail in other articles [20].

2. Experimental

2.1. The cleaning of the substrate

In the experiments, both the glass slides and FTO (20 mm × 20 mm) were used. These slides were immersed into hydrochloric acid (10 wt%) for 30 min, then cleaned with acetone, distilled water, ethanol in an ultrasonic cleaner in turn for 10 min.

2.2. Preparation of the ZnO seed layer

All chemical reagents in the experiment were of analytical grade (AR) and used without further purification. Typically, 1.97 g of diethanolamine ($HN(CH_2CH_2OH)_2$) and 8.23 g of zinc acetate dihydrate ($Zn(CH_3COO)_2{\cdot}2H_2O$) were dissolved in 50 ml of ethylene glycol monomethylether ($CH_3OCH_2CH_2OH$), respectively, to get zinc oxide colloid after the mixture was maintained at 60 °C under magnetic stirring for 2 h. The as-prepared zinc oxide colloid solution was spin-coated on the pretreated glass slides and the FTO substrates, respectively. After coating, these substrates were pre-

* Corresponding author. Tel.: +86 21 52411620; fax: +86 21 52416360.
E-mail address: Huangfq@mail.sic.ac.cn (F. Huang).

0925-8388/$ – see front matter © 2009 Elsevier B.V. All rights reserved.
doi:10.1016/j.jallcom.2009.09.156

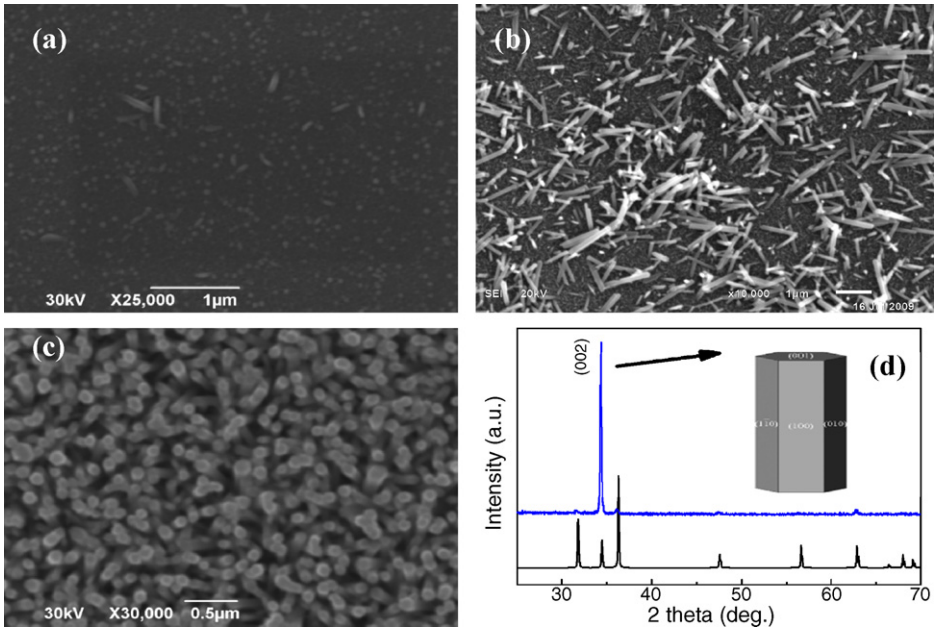

Fig. 1. (a) SEM image of the ZnO seed layer, (b) SEM image of the ZnO nanorods prepared on the glass slide without the seed layer, (c) SEM image of the ZnO nanoarrays prepared on the glass slide with the seed layer, (d) upper curve: XRD pattern of the ZnO nanoarrays and lower curve: the standard XRD pattern of wurtzite ZnO (JCPDS No. 36-1451).

annealed at 300 °C for 10 min and post-annealed at 500 °C for 1 h. After repeating the process of spin-coating and annealing for several times, the zinc oxide seed layer was prepared.

2.3. Growth of ZnO nanoarrays

The growth of ZnO nanoarrays was carried out in the zinc precursor solution by a CBD method. In a typical experiment, an equimolar (0.025 M) aqueous solution of zinc nitrate ($Zn(NO_3)_2{\cdot}6H_2O$) and hexamethylenetetramine ($C_6H_{12}N_4$) was prepared for the growth of ZnO nanoarrays. Similarly, equimolar aqueous solutions of $Zn(NO_3)_2$ and $C_6H_{12}N_4$ with concentrations of 0.050 M and 0.100 M were obtained. The substrates deposited with zinc oxide seed layer were put into the precursor solutions, and then were sealed in a bottle and heated at 95 °C for 6 h. After deposition, the samples were cleaned with distilled water several times and allowed to dry in air.

Similarly, ZnO seed layer substrates were immersed into the 0.05 M precursor solutions at the same temperature but under magnetic stirring for 0 h, 1 h, 2 h, 3 h, 4 h, 5 h and 6 h, respectively. After deposition, the samples were cleaned with distilled water for several times and dried in air.

2.4. Construction of dye-sensitized solar cell

ZnO nanoarrays were grown on the fluorine-doped SnO_2 conducting glass (FTO, Pilkington, 2.2 mm thickness, 15 Ω/□) instead of the glass substrate. FTO was used as current collector. The ZnO nanoarrays were dried at 80 °C for 15 min and then immersed into 0.3 mM dye solution (Solaronix, Z907 dissolved in ethanol) and kept at room temperature for 12 h to assure completely dye uptake. The counter Pt-electrode was obtained by coating with a drop of H_2PtCl_6 solution (5 mM isopropanol solution) on the FTO glass and heated at 300 °C for 15 min. The dye-covered ZnO electrode and Pt-counter electrode were assembled into a sandwich type cell. The electrolyte solution was composed of 0.1 M LiI, 0.05 M I_2, 0.3 M 1,2-dimethyl-3-propyl imidazolium iodine, and 0.5 M tert-butylpyridine in 3-methoxypropionitrile. Then, the DSC cell was obtained.

2.5. Characterization

X-ray diffraction (XRD) patterns were recorded on an X-ray diffraction system (XRD, Rigaku D/Max2550V diffractometer with Cu Kα radiation). The morphology was observed by scanning electron microscopy (SEM JEOL JSM-6510) with an accelerating voltage of 30 kV. Optical transmittance was examined by a UV–vis spectrophotometer (U-3010, Hitachi).

Photovoltaic measurements were employed through a 1000 W Oriel solar simulator (equipped with an AM1.5 filter) by scanning an external bias voltage while measuring the photocurrents. The power of the light was calibrated to 100 mW/cm^2 by using a calibrated Si cell.

3. Results and discussion

3.1. Mechanism for the growth of ZnO nanoarrays by CBD

The zinc oxide seed layer is important for the growth of well-aligned zinc oxide nanoarrays [21]. There exist various techniques for preparing the seed layer including ultrasonic spray pyrolysis [22], pulsed laser deposition [23], and the sol–gel method [24]. In this work, the seed layer was prepared by the sol–gel method of spin-coating. Fig. 1a shows the SEM image of the zinc oxide seed layer, where the seed layer consists of lots of ZnO nanoparticles. After being annealed at 300 °C for 10 min, the combination of chemical bonds between the seed layer and the substrate was formed. This procedure not only made the seed layer have the good crystallinity but also removed the organic substances residual on the substrates which could be from the reagents such as diethanolamine and ethylene glycol monomethylether. After that, the substrate is further annealed at 500 °C. The effect of substrate annealing is investigated by Guo et al. [25]. If the substrates without annealing had been used to grow ZnO nanorods, a poor alignment of the ZnO rods was observed. The high temperature annealing can improve the alignment of the nanoarray. The advantage of the seed layer is that the interface energy between zinc oxide crystal and the substrate can be decreased significantly and the nanoarrays can grow more easily. On the other hand, zinc oxide nanorods could grow into well-aligned nanoarrays in the presence of the seed layer (Fig. 1c). On the contrary, without the seed layer, zinc oxide nanorods grew randomly on the substrate (Fig. 1b). The reason for preparing well-aligned nanoarrays in the presence of the seed layer is based on the fact that the crystal structure of the seed layer is the same as that of zinc oxide nanoarrays. Such a coincidental matchup makes the epitaxial growth of zinc oxide nanorods along the [0 0 0 1] direction of the seed layer on the substrate [26]. Fig. 1d shows the XRD pattern of the zinc oxide nanoarrays (top) prepared from 0.050 M precursor without stirring and the standard XRD pattern of wurtzite zinc oxide (JCPDS No. 36-1451) (down). In nanoarrays the strongest peak corresponds to the (0 0 0 1) plane of the zinc oxide crystal, and differs from the standard pattern of the

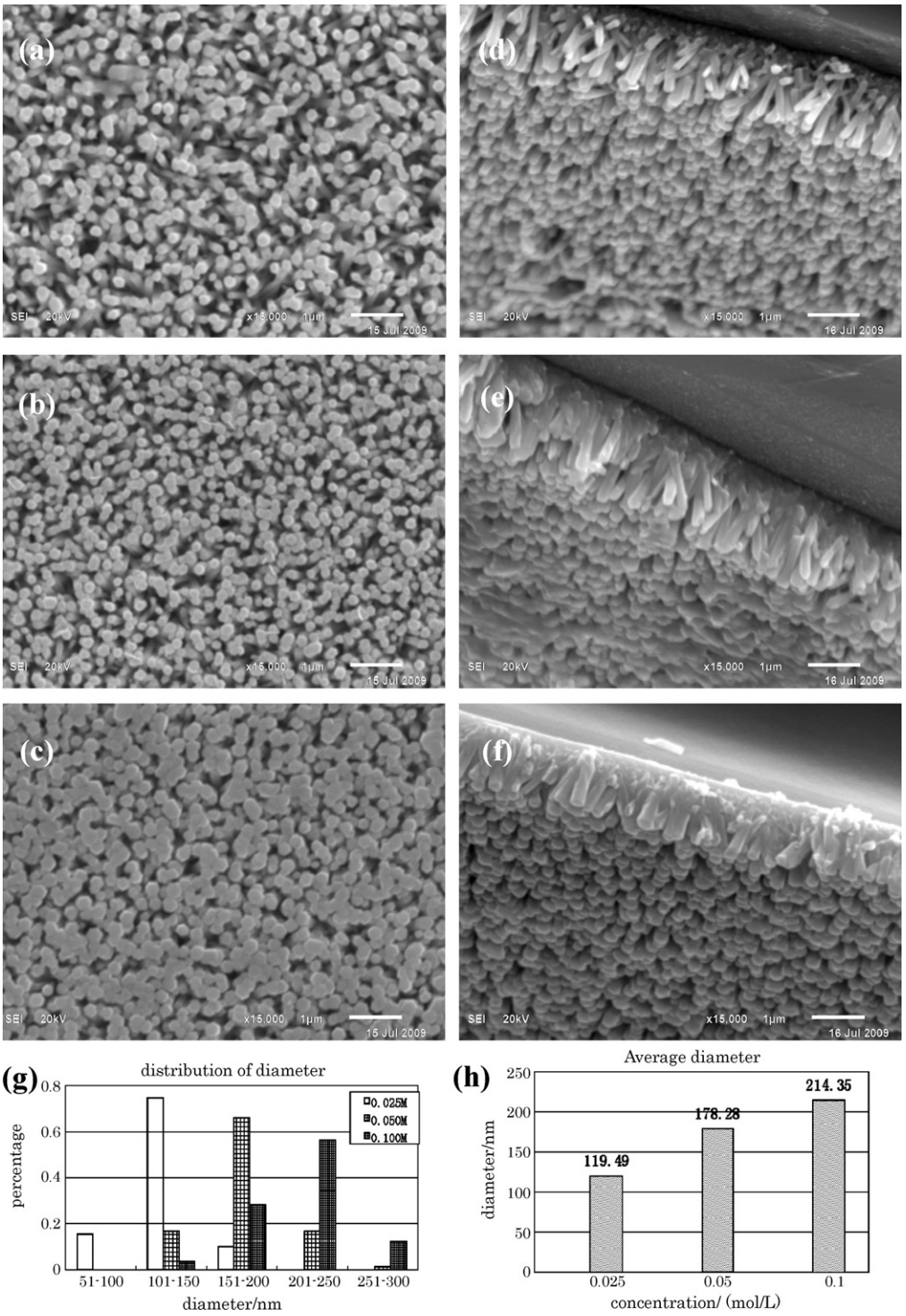

Fig. 2. SEM images of ZnO nanoarrays with different precursor concentrations: (a) 0.025 M; (b) 0.050 M and (c) 0.100 M. Cross-sectional SEM images of ZnO nanoarrays: (d) 0.025 M; (e) 0.050 M and (f) 0.100 M. The diameter distributions of the nanoarrays from different concentrations (g) and the average diameter (h).

bulk material, which is caused by preferred orientation of the as-prepared sample. Also, the sharp diffraction peak of ZnO nanoarrays indicates the good crystallinity of the as-prepared sample.

The growth temperature of 95 °C under boiling point was chosen because the reaction rate can be greatly enhanced at a high temperature in aqueous solution. In the reaction for growing the zinc oxide nanoarrays, hexamethylenetetramine was used as the alkali to provide the OH^- ion slowly, and the zinc nitrate was used as the source of Zn^{2+} ion. The main chemical reaction process can be described as follows:

$$C_6H_{12}N_4 + 6H_2O \rightarrow 6HCHO + 4NH_3 \quad (1)$$

$$NH_3 + H_2O \rightarrow NH_4^+ + OH^- \quad (2)$$

$$2OH^- + Zn^{2+} \rightarrow Zn(OH)_2 \quad (3)$$

$$Zn(OH)_2 \rightarrow ZnO + H_2O \quad (4)$$

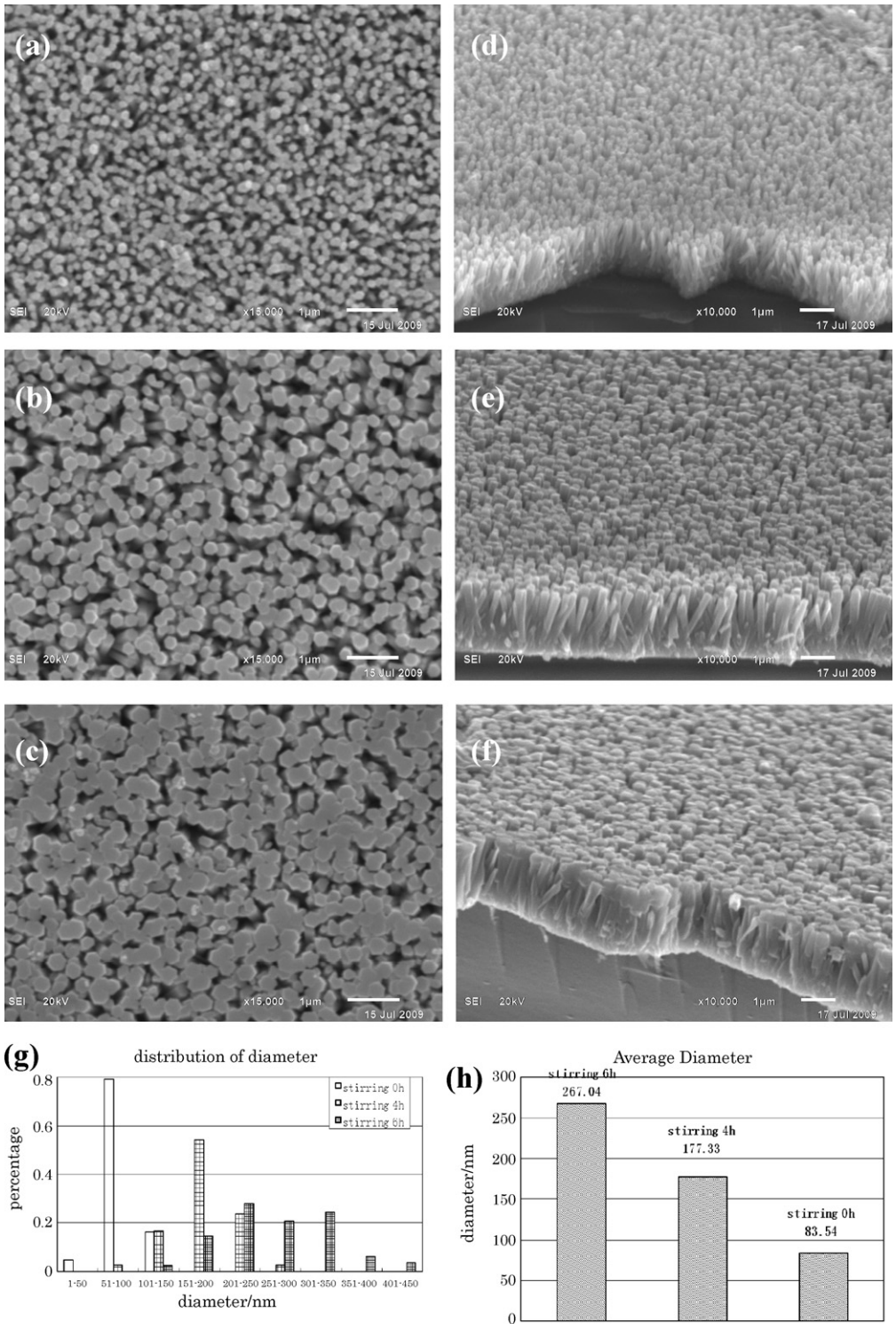

Fig. 3. SEM images of ZnO nanoarrays with different stirring times: (a) 0 h, (b) 4 h and (c) 6 h. Cross-sectional SEM images of ZnO nanoarrays: (d) 0 h, (e) 4 h and (f) 6 h. And the corresponding diameter distributions of the nanoarrays (g) and the corresponding average diameter (h).

Zinc oxide has three crystal structures, cubic rock salt, cubic zinc blende and hexagonal wurtzite, and the wurtzite structure is the most stable one [27]. From the XRD pattern, the as-prepared sample has the hexagonal wurtzite structure anisotropic along the [0 0 0 1] direction, belonging to the *P*63*mc* space group. The (0 0 0 1) plane of zinc oxide has the maximum surface energy, so along the [0 0 0 1] direction there is the fastest growth rate than that along other directions. As a result, the well-aligned nanorods were formed naturally.

3.2. Size tuning of the ZnO nanoarrays

Through varying the precursor concentrations from 0.025 M to 0.100 M without stirring, the influence of the concentration on the morphology of zinc oxide nanoarrays was revealed. From Fig. 2a–c, we observe that, with the increasing of the concentration, the diameter of the zinc oxide nanoarrays also increased [28]. The average diameters of the as-prepared samples growing from 0.025 M,

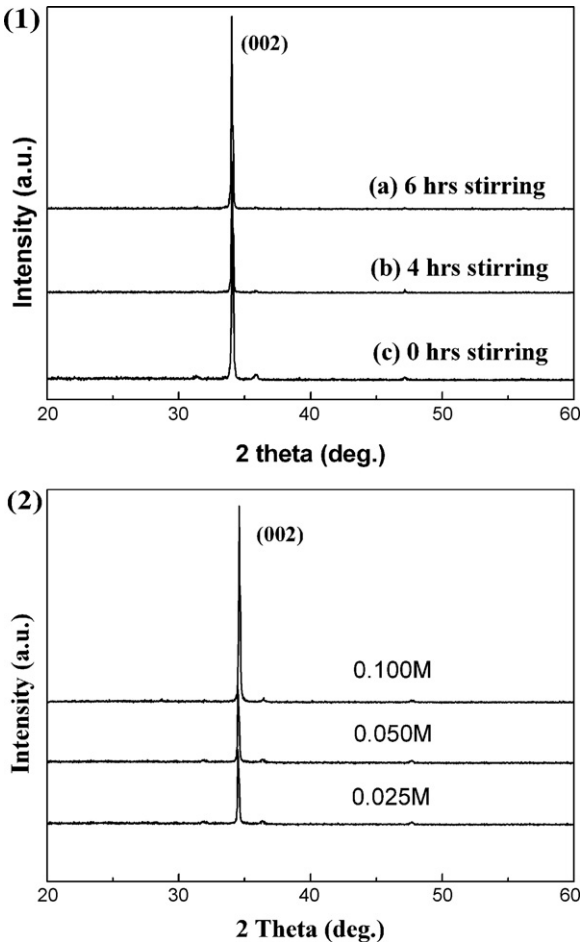

Fig. 4. (1) XRD pattern of ZnO sample prepared from different stirring times: (a) 6 h stirring time; (b) 4 h stirring time and (c) 0 h stirring time. (2) XRD pattern of ZnO sample prepared from different concentrations: (a) 0.100 M; (b) 0.050 M and (c) 0.025 M.

0.050 M, and 0.100 M are 119 nm, 178 nm and 214 nm, respectively (Fig. 2g and h). The cross-sectional images of the samples with different stirring times are shown in Fig. 2d–f. The thickness of samples containing both the seed layer and nanoarrays is about 1.5 μm. Fig. 4(2) shows the XRD patterns of ZnO nanoarrays prepared from different concentrations. Congruously, at about 34.5°, all the three curves present the strongest peak.

So far, many methods are reported to synthesize the zinc oxide nanoarrays in the motionless aqueous solution. However, the growth of zinc oxide nanoarrays in the motional aqueous solution has rarely been reported. In this work, the influence of the stirring on the morphology of zinc oxide nanoarrays was investigated. With the increase of the stirring time while the concentration of precursors is kept at 0.05 M, the density and diameters of zinc oxide nanorods also increased (Fig. 3a–c). The average diameters of the nanoarrays with the stirring time of 0 h, 4 h, and 6 h are 83 nm, 177 nm and 267 nm, respectively (Fig. 3g and h). The cross-sectional images of the samples with different stirring times are shown in Fig. 3d–f. The thickness of samples containing the seed layer and nanoarrays is about 1.5 μm. Fig. 4(1) shows the XRD patterns of ZnO nanoarrays prepared from different stirring times. Also, uniformly, all the three curves have the strongest peak at about 34.5°.

From the transmission spectra (Fig. 5), in the visible light (from 400 nm to 800 nm) high transmissions can be observed for both ZnO seed layer and ZnO nanoarray. In the ultraviolet light (from 250 nm to 400 nm), however, the transmissions of nanoarray ZnO is almost zero, lower than that of ZnO seed layer because the nanoarrays is

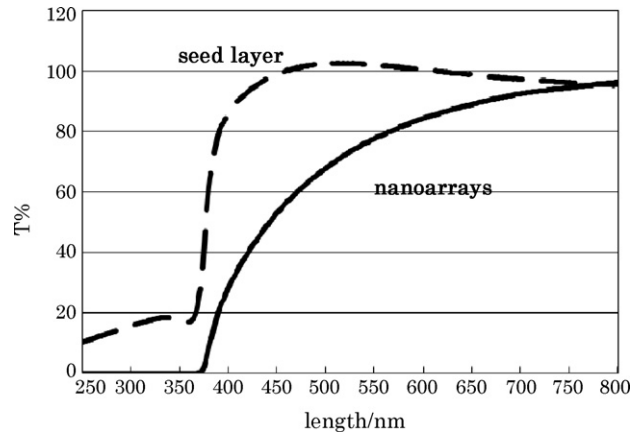

Fig. 5. UV–vis spectrum of the seed layer (dashed curve) and the as-prepared ZnO nanoarrays (solid curve).

thicker than the seed layer and can restrain more light through the samples. The high transmission in the visible light region is one of the reasons that zinc oxide nanoarrays can be used to be the conduction paths for the electrons in the dye-sensitized solar cell without response to the incident light.

3.3. Application of ZnO nanoarrays in DSC

The current–voltage characteristics for the zinc oxide nanoarrays-based dye-sensitized solar cell with illumination from a tungsten lamp are shown in Fig. 6. The open circuit voltage is 0.28 V with illumination while it is 0.16 V in the dark. One of the possible reasons for the low performance of the as-prepared DSSC is that the combination between the dye and ZnO nanoarrays is very poor. As well known, electric current is produced based on the fact that the electrons from the excited-state dye are injected into ZnO nanoarrays connecting with FTO so that these electrons can be guided to the electrode, then to the external circuit. The poor combination between the dye and ZnO nanoarrays will weaken the transferring of electrons, and might lead to recombination between electrons from the dye and triiodide ions in the electrolyte. Another possible reason is the lower surface area as compared to compacted nanoparticles. Besides, that the absolute dark circumstance cannot be obtained led to the leakage current. Although the voltage is low compared with others reported, at

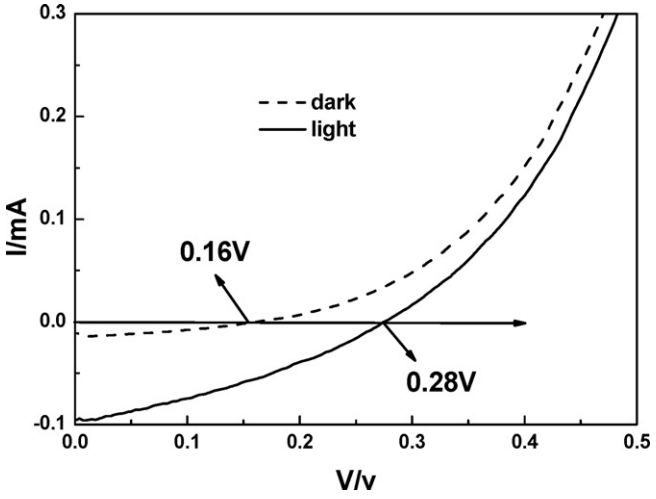

Fig. 6. Current–voltage characteristic of the dye-sensitized solar cell based on ZnO nanoarrays in the dark and with visible illumination.

least it was substantiated that the response to voltage exists. So it is feasible to construct the dye-sensitized solar cell with ZnO nanoarrays. Experiments are in progress to optimize the synthesizing conditions to improve the performance of the device.

4. Conclusions

In summary, it has been shown that zinc oxide nanoarrays could be synthesized by the chemical bath deposition with the spin-coated seed layer. Through varying the concentration of the precursor solution and the stirring time, the size of the nanoarrays diameter was tuned successfully. The morphology is sensitive to the conditions of the preparation process. Current–voltage characteristic shows the potential applications in the dye-sensitized solar cells of such ZnO nanoarrays.

Acknowledgements

This research was financially supported by National 973 Program of China Grant 2007CB936704, National Science Foundation of China Grant 50772123, Science and Technology Commission of Shanghai Grant 0752nm016, and Shanghai Fundamental Research Grant 05JC14080.

References

[1] N. Katsarakis, N. Katsarakis, M. Bender, V. Cimalla, E. Gagaoudakis, G. Kiriakidis, Sens. Actuators B: Chem. 96 (2003) 76–81.
[2] J.B. Baxter, E.S. Aydil, Appl. Phys. Lett. 86 (2005) 053114.
[3] Z.L. Wang, J.H. Song, Science 312 (2006) 242–246.
[4] J.C. Johnson, H. Yan, R.D. Schaller, L.H. Haber, R.J. Saykally, P. Yang, J. Phys. Chem. B 105 (2001) 11387–11390.
[5] T. Izumi, K. Izumi, N. Kuroiwa, A. Senjuh, A. Fujimoto, M. Adachi, T. Yamamoto, J. Alloys Compd. 480 (2009) 123–125.
[6] Z.W. Pan, Z.R. Dai, Z.L. Wang, Science 291 (2001) 1947–1949.
[7] X.Y. Kong, X.Y. Kong, Y. Ding, R. Yang, Z.L. Wang, Science 303 (2004) 1348–1351.
[8] P.X. Gao, P.X. Gao, Y. Ding, W. Mai, W.L. Hughes, C. Lao, Z.L. Wang, Science 309 (2005) 1700–1704.
[9] Y.J. Xing, Z.H. Xi, Z.Q. Xue, X.D. Zhang, J.H. Song, R.M. Wang, J. Xu, Y. Song, S.L. Zhang, D.P. Yu, Appl. Phys. Lett. 83 (2003) 1689–1691.
[10] W.I. Park, D.H. Kim, S.W. Jung, G.C. Yi, Appl. Phys. Lett. 80 (2002) 4232–4234.
[11] M.H. Huang, S. Mao, H. Feick, H. Yan, Y. Wu, H. Kind, E. Weber, R. Russo, P. Yang, Science 292 (2001) 1897–1899.
[12] W.I. Park, G.C. Yi, M. Kim, S.J. Pennycook, Adv. Mater. 14 (2002) 1841–1843.
[13] Y. Li, G.W. Meng, L.D. Zhang, Appl. Phys. Lett. 76 (2000) 2011–2013.
[14] X.F. Duan, C.M. Lieber, Adv. Mater. 12 (2000) 298–302.
[15] S.M. Rozati, S. Akeste, Cryst. Res. Technol. 43 (2008) 273–275.
[16] J.D. Holmes, K.P. Johnston, R.C. Doty, B.A. Korgel, Science 287 (2000) 1471–1473.
[17] W.Q. Peng, S.C. Qu, G.W. Cong, Z.G. Wang, Cryst. Growth Des. 6 (2006) 1518–1522.
[18] I. Gonzalez-Valls, M. Lira-Cantu, Energy Environ. Sci. 2 (2009) 19–34.
[19] C.D. Lokhande, P.M. Gondkar, R.S. Mane, V.R. Shinde, S.H. Han, J. Alloys Compd. 475 (2009) 304–311.
[20] J.K. Chen, K.X. Li, Y.H. Luo, X.Z. Guo, D.M. Li, M.H. Deng, S.Q. Huang, Q.B. Meng, Carbon 47 (2009) 2704–2708.
[21] Y.H. Tong, Y. Liu, L. Dong, D. Zhao, J. Zhang, Y. Lu, D. Shen, X. Fan, J. Phys. Chem. B 110 (2006) 20263–20267.
[22] J.M. Bian, X.M. Li, X.D. Gao, W.D. Yu, L.D. Chen, Appl. Phys. Lett. 84 (2004) 541–543.
[23] X.W. Sun, H.S. Kwok, J. Appl. Phys. 86 (1999) 408–411.
[24] V.S. Raja, S. Jeevanandam, L.G. Bhatgadde, J. Mater. Sci. Lett. 16 (1997) 417–419.
[25] M. Guo, P. Diao, S.M. Cai, J. Solid State Chem. 178 (2005) 1864–1873.
[26] Y. Sun, G.M. Fuge, N.A. Fox, Adv. Mater. 17 (2005) 2477–2481.
[27] Ü. Özgür, Ya.I. Alivov, C. Liu, A. Teke, M.A. Reshchikov, S. Doğan, V. Avrutin, S.-J. Cho, H. Morkoc, J. Appl. Phys. 98 (2005) 041301.
[28] L. Vayssieres, Adv. Mater. 15 (2003) 464–466.